Low-Profile Patch Antennas for Over-Body-Surface Communication at 2.45 GHz

Gareth A. Conway* & William G. Scanlon

Institute of Electronics, Communications & IT, Queen's University Belfast, Belfast, BT3 9DT.
Email: gconway03@ecit.qub.ac.uk; w.scanlon@ qub.ac.uk

ABSTRACT

Two low-profile patch antennas on small ground planes (0.25 λ), suitable for over the body surface communication at 2.45 GHz are presented. On-Body performance was investigated using FDTD simulations of S_{21} coupling of shorted microstrip patch antennas (S-MPA) and higher-order mode microstrip patch antennas (HM-MPA) placed on numerical tissue phantoms with characteristics of muscle tissue. The low-profile antenna coupling results are comparable to those achieved using a quarter wave monopole antenna on the same size of groundplane, mounted normal to the tissue surface, indicating that the low-profile antennas studied are promising for bodyworn antenna applications.

INTRODUCTION

Close proximity to the human body presents a challenging environment for antennas, with a strong influence on both channel and antenna characteristics. Key antenna characteristics are significantly affected by coupling to the lossy dielectric body tissues including radiation efficiency, resonant frequency, feed-point impedance and radiation pattern fragmentation [1]. Furthermore, these effects depend on the antenna design, separation distance and groundplane / counterpoise characteristics. Emerging Wireless Personal Area Network (WPAN) applications are focused on integrating wireless communication systems into close fitting clothing. An important aspect of these systems is the preservation of antenna performance, yet antennas must be small, unobtrusive to the user and, ideally conformable to the body surface. As antenna size is a critical design criterion for wearable applications, groundplane dimensions must also be minimised, further compounding the antenna-body effect.

To date there has been no significant breakthrough in the design of low-profile body-mounted antennas but studies of wearable antennas have recently received much attention [2]. In this paper we look at the performance of a shorted microstrip patch antenna (S-MPA) and a higher mode microstrip patch antenna (HM-MPA) both with relatively small (0.25 λ) groundplanes for over the body surface communication (an 'on-body' channel) at 2.45 GHz. The 2.45 GHz band is popular for on-body communications because of commercial WPAN standards such as Zigbee IEEE 802.15.4 and Bluetooth IEEE 802.15.1. We report simulated S_{21} coupling performance for the S-MPA and HM-MPA in close proximity to a lossy medium representing body tissues. The results are compared to a λ/4 monopole antenna mounted normal to the tissue surface and on the same size of groundplane. All simulated results in this work were obtained with the SEMCAD X finite-difference time-domain (FDTD) electromagnetic numerical modelling platform.

ON-BODY CHANNEL

On-body channels exist where there is a need for communication between devices located on, or within, the user's body. For example, in telemedicine applications a wireless body area network consisting of several wearable biosensors communicating with a bodyworn controller, which often also acts as a relay to a remote station. In anechoic environments electromagnetic wave propagation around the body is restricted to two mechanisms. At UHF and above, penetration through the body is significantly reduced and the main mechanism for propagation around the body is via a creeping Zenneck-type wave [3]. Therefore, a compact low-profile antenna that radiates maximum power tangential to the body surface is required to maximise coupling between bodyworn devices. If two antennas are placed on the body in an arrangement that eliminates the line-of-sight propagation path, the creeping wave will be the only propagation mechanism in open, reduced multipath environments. For example, a measurement scenario where two antennas are placed on opposite sides of the body torso would best evaluate an antenna's effectiveness at maximising the creeping wave mechanism essential for improving over-body surface communication.

ANTENNA STRUCTURE

Fig. 1 shows the geometry of both antennas and principal dimensions for free-space and tissue mounted operation at 2.45 GHz are shown in Table 1. The band is centred at 2442 MHz, with an antenna bandwidth requirement of 4 % (84 MHz). The S-MPA patch and groundplane metallization (Fig. 1 (a)) were modelled on PTFE substrates with a permittivity of 2.33 (ε_{r1}, Taconic TLY-3) and 6.15 (ε_{r3}, Taconic RF-60A). A low permittivity (ε_{r2} = 1.07) Rohacell 31 HF polymethacrylimide foam spacer was used to increase antenna bandwidth. The patch element was shorted to ground via a shortening strip to reduce the dimensions of the antenna. Further size reduction may be realised using a shortening post as apposed to a shortening strip, but at the expense of reduced bandwidth. The HM-MPA (Fig. 1 (b)) consists of a groundplane and patch metallization on a dielectric substrate with a permittivity of 2.33 (ε_{r1}, Taconic TLY-3). The antenna is excited by a probe at the centre of the patch element [4]. Two posts offset from the feed and shorted to ground are used to force nulls in the tangential electric field component between the groundplane and patch element, exciting a second or higher order resonant mode (TM^{z}_{21}).

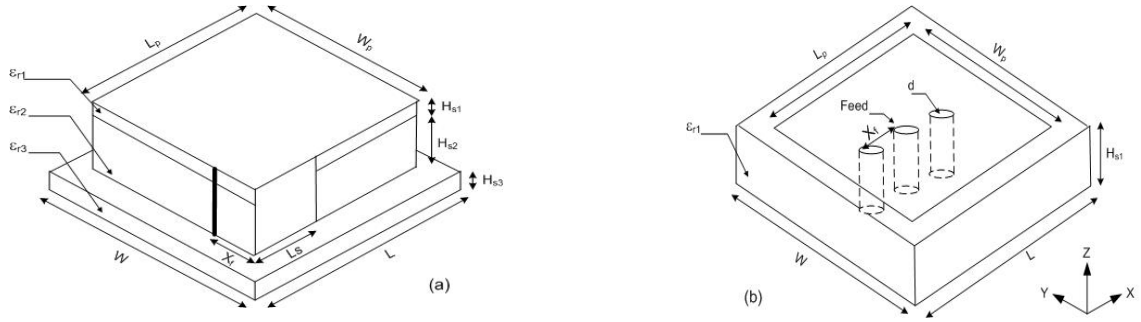

Fig. 1 Antenna geometries: (a) S-MPA (b) HM-MPA.

Tab. 1 Principal antenna dimensions for free-space and tissue mounted operation at 2.45 GHz.

Antenna	Location	Antenna Dimensions (mm)								Substrate		
		W	L	W_p	L_p	X_f	L_s	H_{s1}	H_{s2}	H_{s3}	ε_{r1}	ε_{r2}	ε_{r3}
S-MPA	Free-Space	30.0	30.0	**14.5**	**14.5**	**4.0**	3.0	0.5	9.0	0.5	2.33	1.07	6.15
S-MPA	Tissue	30.0	30.0	**16.0**	**16.0**	**12.0**	3.0	0.5	9.0	0.5	2.33	1.07	6.15
HM-MPA	Free-space	30.0	30.0	**16.0**	**16.0**	**3.3**	--	10.0	--	--	2.33	--	--
HM-MPA	Tissue	30.0	30.0	**18.0**	**18.0**	**6.3**	--	10.0	--	--	2.33	--	--

The dielectric properties of biological tissues vary with both tissue type and frequency, and in this paper phantom permittivity and conductivity were chosen to represent muscle tissue at 2.45 GHz (ε = 53.58, σ = 1.81 S^{-1}). Fig. 2 shows the simulated return loss for the S-MPA and HM-MPA antennas under both free space and tissue mounted (1-mm separation from a 30 mm thick slab phantom) conditions. The S-MPA was tuned to be resonant at 2.45 GHz on the tissue by moving the location of the probe feed along the edge of the patch. The HM-MPA was tuned by adjusting the distance of the ground posts from the centre feed (Table 1). Table 2 shows free-space and tissue mounted bandwidth and efficiency results for both patch antennas and a reference $\lambda/4$ monopole. The HM-MPA had lower radiation efficiency than the S-MPA as there were increased substrate losses due to increased permittivity. The impedance bandwidth of all antennas increased when on-tissue. This bandwidth enhancement is due to the increased coupling losses associated with the lossy medium lowering the antenna Q factor.

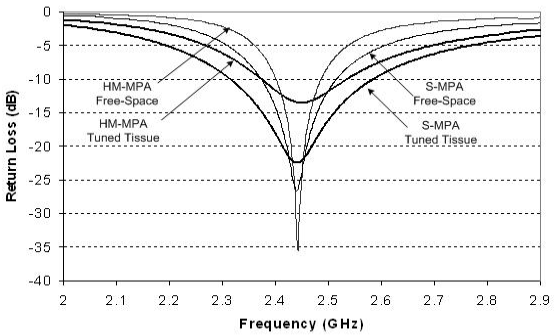

Fig. 2 S_{11} for S-MPA and HM-MPA in free-space and mounted 1-mm from muscle tissue.

Tab. 2 Free-space and tissue proximity efficiency results at 2.45 GHz

Antenna	Location	Bandwidth (VSWR<2.0, MHz)	Efficiency (%)	Dielectric & tissue losses
Monopole	Free-space	--	99	
	Tissue	343	71	1.5 dB
S-MPA	Free-space	143	98	
	Tissue	264	64	1.9 dB
HM-MPA	Free-space	86	93	
	Tissue	165	62	2.1 dB

COUPLING RESULTS ACROSS A FLAT NUMERICAL PHANTOM

The on-body coupling (S_{21}) performance of the S-MPA and HM-MPA was compared to a reference monopole antenna. The monopole was modelled as a 0.24 λ PEC wire with a diameter of 0.5 mm mounted on same size of groundplane. In the simulation setup (Fig. 3), the antennas were spaced 1 mm above and placed 200 mm apart on a flat tissue phantom with dimensions 580 x 380 mm. Larger phantoms did not yield substantially more accurate results for increase in computational resource and simulation time. For example, increasing all phantom dimensions by a factor of 2 gave a 0.6 dB change in peak S_{21} values. The transmit antenna (Tx) was excited by voltage source (1 V, impedance 50Ω). At the receive antenna (Rx) a pure resistive load was place between the antenna and ground. Sensors at the source and load recorded voltage and current as a function of frequency for extracting S_{21}. The tissue phantom had a thickness of 30 mm, larger than the maximum signal penetration depth of muscle tissue at 2.5 GHz [1].

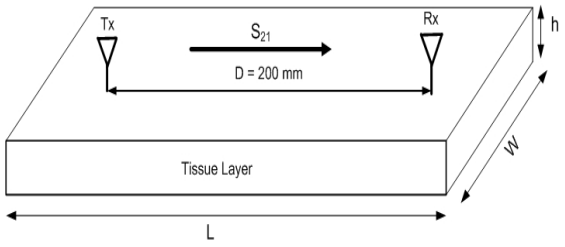

Fig. 3 Antenna coupling simulation setup.

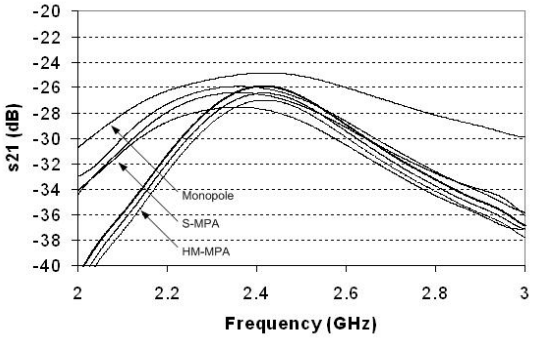

Fig. 4 Simulated S_{21} coupling for S-MPA and HM-MPA versus monopole reference antenna.

Fig. 4 compares the S_{21} coupling of two S-MPA and HM-MPA antennas for different orientations (detailed in Fig. 5), with two monopole antennas placed 200 mm apart on the tissue layer described above. As the MPA's do not radiate uniformly in the XY plane (azimuth), S_{21} coupling results were recorded for each possible orientation combination, the best, median and worst orientation case have been reported here. The results (Table 3) show that for orientation scenarios (a) and (d), both of the new low-profile antennas have only 1 dB more coupling loss than a monopole for this 'on-body' link, as represented by the muscle-equivalent tissue slab. This coupling difference may be further reduced by increasing radiation along the tissue surface or improving the low-profile antenna efficiency, more so for the HM-MPA antenna where substrate dielectric losses were 7 % (Table 2).

Tab. 3 Summary of S_{21} coupling results of MPA's versus Monopole.

Antenna	Orientation	Peak $\|S_{21}\|$ (dB)	$\|S_{21}\|$ over 3 dB Bandwidth	3 dB Bandwidth
Monopole	-	–25.0	–28.0	683 MHz
S-MPA	a	–25.9	–28.9	478 MHz
	b	–26.4	–29.4	470 MHz
	c	–27.5	–30.5	482 MHz
HM-MPA	d	–26.0	–29.0	348 MHz
	e	–26.5	–29.5	349 MHz
	f	–27.0	–30.0	345 MHz

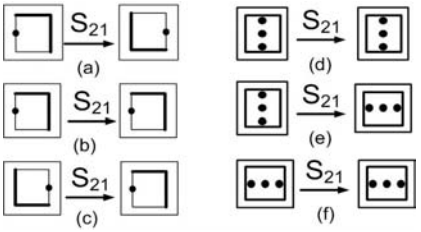

Fig. 5 Antenna orientations: (a-c) S-MPA (d-f) HM-MPA.

COUPLING RESULTS AROUND A CYLINDRICAL NUMERICAL PHANTOM

To investigate antenna coupling performance in terms of creeping waves, the antennas (S-MPA and HM-MPA in orientations (a) and (d), respectively) were placed on opposite sides of a 3D phantom (Fig. 6), removing the line-of-sight propagation path. A phantom thickness of 100 mm was chosen to eliminate signal penetration through the tissue model, effectively isolating the creeping wave propagation mode. The antennas were spaced 1 mm from the numerical phantom with dimensions 50, 100, 400 mm (L, r, W), respectively. The normalised E-field magnitude in the YZ plane through the TX antenna feed point is shown in Fig. 7. The surface propagating wave close to the body surface is diffracted around the body due to body coupling, which excites the receive antenna. The results (Table 4) show that the HM-MPA had better S_{21} coupling performance than the S-MPA but it still was 1.5 dB worse than the monopole

reference antenna. However, the monopole and HM-MPA had total tissue proximity losses of 3 dB and 4.2 dB, respectively (2 antennas in each scenario). By subtracting total dielectric losses (tissue plus substrate) from the S_{21} results, it was estimated that the HM-MPA had a 0.3 dB greater coupling loss over the monopole for this 'on-body' link. The results also show that the peak S_{21} results were reduced by approximately 15 dB compared to those on a flat phantom. This difference is a combination of an increase in propagating distance between the antennas (57 mm) and, to a larger extent, the removal of the line-of-sight propagation mode. Further improvements in over the body surface communication performance will only be seen with antennas that maximise the creeping, surface propagating mode.

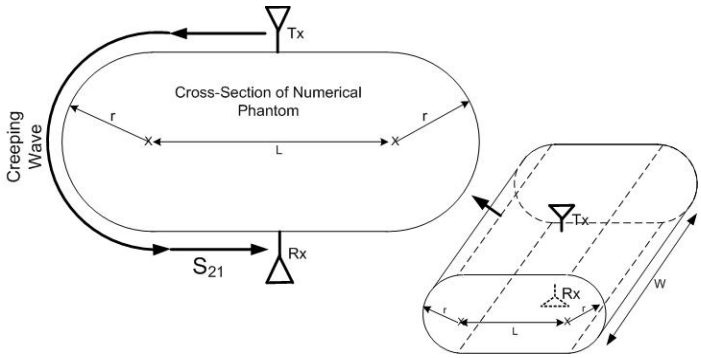

Fig. 6 Antenna coupling simulation setup.

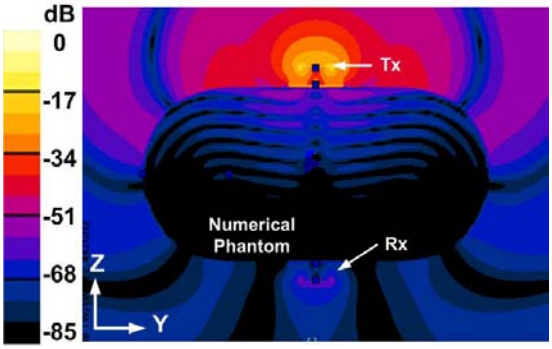

Fig. 7 HM-MPA antenna coupling results showing normalised E-field magnitude through TX feedpoint.

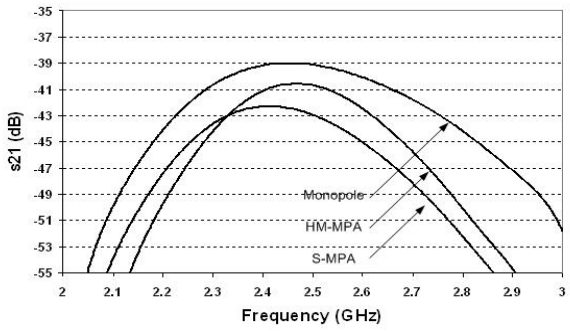

Fig. 8 Simulated S_{21} coupling for MPA's versus monopole.

Tab. 4 Summary of S_{21} coupling results for each antenna.

Antenna	Orientation	Peak $\|S_{21}\|$ (dB)	$\|S_{21}\|$ 3 dB Bandwidth
Monopole	-	–39.0	459 MHz
S-MPA	a	–40.5	366 MHz
HM-MPA	d	–42.3	330 MHz

CONCLUSIONS

The on-body coupling performance of two compact microstrip patch antennas in close proximity to a lossy dielectric medium at 2.45 GHz was studied using FDTD. The low-profile antennas have relatively small groundplanes yet provide comparable performance to a full-size monopole. Furthermore, close proximity to the lossy tissue almost doubled the impedance bandwidth. Future work will include investigation using near-field analysis to improve on-body coupling performance of low-profile antenna structures with a phantom and antenna build to validate simulation results. Antenna height reduction, but with preservation of the impedance bandwidth and surface-wave coupling performance, is another major aim of current work. Alternative microstrip antenna feed techniques such as insert feed and electromagnetically coupled feed must also be investigated for practical wearable system designs.

REFERENCES

[1] W.G. Scanlon and N.E. Evans, "Numerical analysis of bodyworn UHF antenna systems," *IEE Electronics & Communication Engineering Journal*, vol. 13, pp. 53–64, 2001.

[2] K.L. Wong, C.I. Lin. "Characteristics of a 2.4-GHz compact shorted patch antenna in close proximity to a lossy medium," *Microwave and Optical Technology Letters*, vol. 45, Issue 6, pp. 480–483, 2005.

[3] J. Ryckaert, P. De Doncker, R. Meys, A. de Le Hoye and S. Donnay, "Channel model for wireless communication around human body," *IEE Electronics Letters*, vol. 40, pp. 543–544, April, 2004.

[4] C. Delaveaud, P. Leveque, and B. Jecko, "New kind of microstrip antenna: The monopolar wire-patch antenna," *Electron. Lett.*, vol. 30, pp. 1–2, Jan. 1994.